Progress In Electromagnetics Research, Vol. 116, 347–361, 2011

AN ARTIFICIAL NERVE NETWORK REALIZATION IN THE MEASUREMENT OF MATERIAL PERMITTIVITY

Q. Chen, K.-M. Huang, X. Yang, M. Luo, and H. Zhu

School of Electronics and Information Engineering
Sichuan University, Chengdu 610064, China

Abstract—Effective complex permittivity measurements of materials are important in microwave engineering and microwave chemistry. Artificial neural network (ANN) computational module has been used in microwave technology and becomes a useful tool recently. A neural network can be trained to learn the behavior of an effective permittivity of material under microwave irradiation in a test system, and it can provide a fast and accurate result for the permittivity measurement of material. Thus, an on-line measurement has been realized. This paper presents a simple and convenient reconstruction algorithm for determining the dielectric properties of materials. First, a measurement system is designed, and the reflection coefficient is calculated by employing full-wave simulations. Second, an artificial nerve network has been applied, and adequate simulated materials are utilized to train the networks. Last, the trained network is employed to reconstruct the effective permittivity of several organic solvents using the measured scattering parameters, and the reconstructed results for several organic solvents agree well with reference data and the relative errors between them are less than 5%.

1. INTRODUCTION

Effective permittivity measurements of materials are important in microwave engineering, microwave material processing, microwave chemistry, and electrobiology [1–3]. For this reason, various microwave techniques have been introduced to characterize the electrical properties of materials. These methods can roughly be divided into resonant and non-resonant methods [4]. Resonant

Received 29 January 2011, Accepted 26 April 2011, Scheduled 9 May 2011
Corresponding author: Kama Huang (kmhuang@scu.edu.cn).

methods have much better accuracy and sensitivity than non-resonant methods [5]. Moreover, the perturbation method associated with the measurement of resonant frequencies and the Q-factor of a cavity can give satisfactory results, but even the advanced variants of this method (for example, [6]) have a principal limitation: The sample size should be very small compared to the dimension of the cavity so that the electric field inside the cavity does not change much due to the presence of the sample. Also, the sample must be of a specified shape for which corresponding formulas computing permittivity are eligible. In many applications, these requirements are difficult to follow or simply not acceptable. On the other hand, non-resonant methods have relatively higher accuracy over a broad frequency band and necessitate less sample preparation than resonant methods [7]. Due to their relative simplicity, non-resonant waveguide coaxial transmission/reflection methods are presently the most widely used broadband measurement techniques [8]. Various non-resonant transmission-reflection methods have been proposed for electrical characterization of low-, medium-, and high-loss materials [9–18].

Especially, in some chemistry reaction, since the reactants form a complicated mixture, which varies with time, an effective permittivity can be used to describe the molecular polarization of the mixture in the reaction [19]. The effective permittivity is expected to vary with respect to microwave frequency, temperature, and reaction time. An on-line measurement is needed to reconstruct the effective permittivity. However, in many cases, the effective permittivity of chemistry reaction is difficult to be measured on-line with traditional reconstruction algorithms. Artificial neural network computational modules have gained recognition as an unconventional and useful tool for microwave technology recently [20–22].

Neural networks can be trained to learn the behavior of the effective permittivity of the material under microwave irradiation. When the network is sufficiently trained, it is supplied with the values of measured complex S-parameters and determines ε_r' and ε_r'' of the sample. The measurement apparatus in [20] is adapted to measure the liquid materials with high loss factor. The ANN with samples using uniform grid distribution is used to reconstruct the permittivity. Fast, accurate, and reliable neural network models can be developed from measured/simulated microwave data. In [21], an open-ended coaxial probe is used to determine the dielectric properties of materials from uncorrected reflection coefficient measurements by using an artificial neural network. The ANN was trained by using measurements made on several isopropyl alcohol solutions. In [22], a method employing neural

network control over FDTD modeling is proposed for the determination of the permittivity of dielectric materials. The dielectric properties of fresh and saline water at 915 MHz have been obtained.

This paper is concerned with application of an advanced BP neural network optimization technique to measure the permittivity of materials. We present a simple and convenient reconstruction algorithm for determining the effective permittivity. A measurement system has been designed, and the S-parameters are obtained by the frequency dependent finite difference time domain (FDTD) to reconstruct the permittivity of material. Moreover, the normalization has been used to improve the convergence speed in neural networks, and to improve accuracy of the reconstruction result, more training samples have been selected from materials of low permittivity. At last, several organic solvents have been measured. The reconstructed results of the effective permittivities of solvents by means of the ANN agree well with previous published data.

Compared with the measurement methods mentioned above, the measurement technique in this paper has some advantages. The measurement system can operate in a broad frequency band and deal with a temperature rising process; the sample may be liquids, powders or gases. Moreover, the neural model development using simulation data is very convenient.

2. BP ALGORITHM

The back propagation (BP) neural networks have been widely applied in various areas of scientific research and engineering [23]. Among all kinds of artificial neural network studied today, the BP network, which depends on simple structure, strong operation-ability, imitation of every nonlinear relation between input and output, is widely applied in the fields such as function approximation, pattern identification, classification, data compress, image process, system control, etc. [24, 25]. In fact, it is to modify weight coefficient, according to negative grads direction of error function, to make error decrease.

2.1. Diagram of BP Algorithm

The BP network used in this technique is shown in Fig. 1. A BP neural network is a kind of typical forward network, composed of input layer, hidden layer and output layer. Full interconnect form is among the layers. Multilayer perceptions (MLP) are one of the commonly used neural network structure. In a typical (MLP) neural network, each

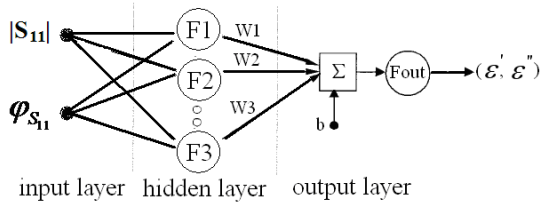

Figure 1. The structure of the BP.

node is connected to all the nodes in the previous layer as well as all the nodes in the next layer. And disconnects form between two neural units of the same layer. BP network transmits directly, and information transmission is bidirectional. In this paper, BP neural network has been used to reconstruct the effective permittivity of material measured by scattering parameter ($|S_{11}|$, $\varphi_{S_{11}}$).

2.2. Fundamental Principle of BP Algorithm [26]

A neural network is created with one or more levels of hidden nodes to model a system. There are multiple connections, which all have the weight and error term adjusted through the training process, from the inputs to the nodes of the hidden layer and, then, to the output. Weights are assigned during training to each arc between the nodes. The node then uses a transfer function to produce a weight-associated output. During the training process, the network assigns weights to the nodes to achieve the best relationship between the training input and output values. The neural network runs through the process many times adjusting weights to minimize the error. Once trained, the network has a model with the weights that provide the best results to calculate the estimate for a part that is not in the training data set [27].

2.3. Reconstruction of Permittivity for Material by BP Network

Figure 2 shows the process to reconstruct the permittivity for material by BP network. The result can be gained very quickly once the network has been trained, because the samples have been produced by FDTD method before trained. Neural model development using simulation data has some advantages: firstly, to sweep any parameter in the simulator is relatively easier; secondly, any response can be modeled as long as it can be computed in the simulator. In this paper, training data is generated with the help of a special procedure which repeatedly

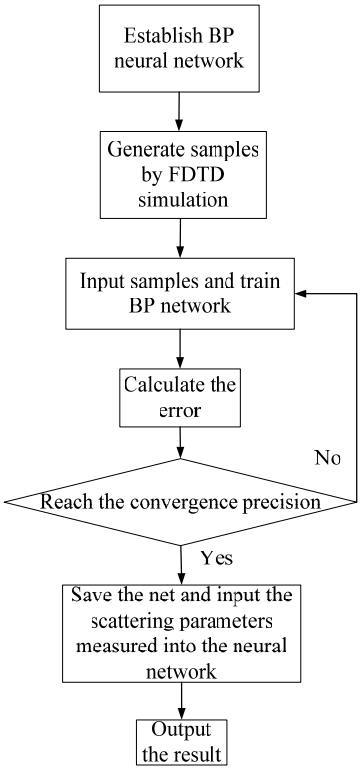

Figure 2. The flow chart of reconstruction permittivity by BP.

operates the (CST) simulation computing the reflection coefficient for different values of permittivity of the sample.

The reconstruction for the permittivity of material with the ANN and FDTD in a broadband measurement is proposed in this paper. The dielectric properties of materials in a broad band are very convenient to obtain, when the permittivity of materials as variables has been simulated in FDTD within the frequency band.

The network has been trained by samples before measurement and saved, then the test data are gotten from measurement. Training technique, namely back propagation is implemented with the use of the gradient method. When the network is sufficiently trained, it is supplied with the values of measured S-parameters and determines ε_r' and ε_r'' of the sample in several seconds. The test data can be processed in parallel. Many reconstruct results can be gained at one time. So the on-line measurement has been realized by using BP neural network.

The computational component of our technique is implemented as a MATLAB code; the N (data of neural) is selected by the existing empirical formulas based on the data of samples. We train 5 times with one structure and save the net structure with the smallest mean square error.

3. MEASUREMENT APPARATUS

In this section, the functionality of the BP algorithm is illustrated by examples. The experimental component of the present method is realized with a transmission-line method. We use a new open ended coaxial probe to measure the magnitude and phase of reflection coefficients ($|S_{11}|$, $\varphi_{S_{11}}$) at the frequency of interest f_0 contained in an iron can structure in this work. The measurement apparatus can be used over a broad frequency band. The measurement installation is shown in Fig. 4. For measuring the permittivity of materials, many structures using coaxial lines have been reported [20, 21, 28]. In [20, 21], the apparatus was used to measure the permittivities of liquid materials. The line was designed for measurements of soil samples in [28]. However, in many cases, the change of the effective permittivity is too small to be observed by traditional methods. We propose an iron can to contain the material measured as in Fig. 7. The sample may be liquids, powders or gases. The inner and outer radii of the iron can are 50 mm and 53 mm, respectively. The height of the iron can is 100 mm. The iron can structure is large enough, so that the

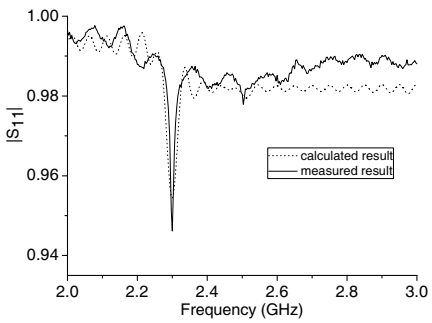

Figure 3. Measurement and simulation magnitude of the reflection coefficient.

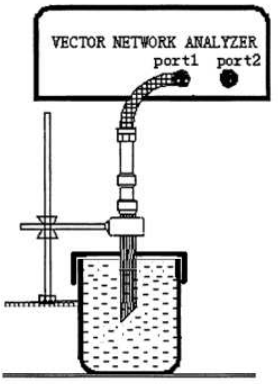

Figure 4. Measurement installation.

Figure 5. Structure of the open ended coaxial probe.

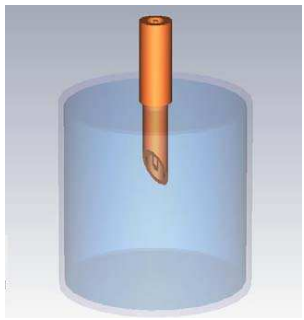

Figure 6. Simulation model.

scattering parameters which are used to reconstruct the permittivity can reflect the dielectric properties of materials measured. The on-line measurement apparatus can be applied to measure the material permittivities in a temperature rising process, because the iron counter could be heated directly and has a better thermal conductive property when the material permittivity in high temperature is measured. Moreover, the coaxial probe has been designed in the pointed-end structure for plugging in powders easily as in Fig. 5. The joint of the probe is designed as type N, the connector commonly used in microwave measurements, to connect with the analyzer easily. To validate the performance of the coaxial structure, the experimental and computational results show that the coaxial probe is very sensitive to the change of the effective permittivity, and the results agree with each other well. The simulation and measurement results for air from 2 GHz to 3 GHz have been obtained. The comparison between the calculated and measured magnitudes of the reflection coefficient are shown in Fig. 3.

In the process, data, which are needed to be trained in networks, and their performance is evaluated, were obtained from simulations accomplished with the FDTD. The simulation model is shown in Fig. 6. Because these materials to be studied are dispersive materials, we develop a MLP neural network based BP arithmetic and use enough simulated materials as samples to train the networks.

4. NORMALIZATION OF THE TRAINING SAMPLES

BP neural network with normalization is measurably superior to the standard online BP algorithm in terms of the convergence speed and accuracy. When facing the original data from simulation, one realizes

that they are expressed in very different units, not even belonging to the same units system. Not only are the units different, but also the order of magnitude of their absolute values are very different. The phase of S_{11}, one of the input data, ranges from $-180°$ to $180°$. However, the other input data $|S_{11}|$ range from 0 to 1. The normalization of data balances the ranges of different inputs.

The most common normalization methods used during data transformation include the min-max, z-score, and decimal scaling [29]. For the min-max and decimal scaling methods, their applicability depends on knowing the minimum and/or maximum values. For the z-score method, in contrast, it is useful when the minimum and maximum values of an attribute are unknown. After the min-max normalization, data values are set between zero and one. However, the z-score and decimal scaling set the data values from -1 to 1 [30]. The min-max scaling method has been used to normalize the training samples.

In this paper, the error precision is 10^{-3}, and the maximal cycle number is 6000. The training process is stopped when either condition is reached. The training of the neural network without normalization of input data is not convergent after 6000 epochs. The number of epochs reaches the value preset, and the training process is stopped. So the neural network maybe use more time to train the network to reach the accuracy predetermined.

We have found that input data normalization with certain criteria prior to a training process is crucial to obtaining good results as well as to significantly accelerate the calculations [31–33].

The neural network has been convergent using the normalization of input data when the number of epochs attains 6000. So the normalization affects the convergence properties of neural network and exhibits a superior performance to the traditional method in terms of convergence speed. Then the anti-normalization must be used when the output data has been obtained form the trained neural network.

5. CONSTRUCTION OF THE SAMPLE SPACE [32]

Data generation is a crucial step toward developing accurate and reliable neural models. Suggested sample distributions are uniform grid distribution, nonuniform grid distribution, star distribution, central-composite distribution, and random distribution [34]. In uniform grid distribution, each input parameter is sampled at equal intervals, while in nonuniform grid distribution, each input parameter is sampled at unequal intervals. Uniform grid distribution could be a default strategy. Nonuniform grid distribution is used when we have a certain understanding of the problem and deliberately choose dense samples

in subregions of the input space where problem behavior is highly nonlinear.

In this section, we describe the creation of the sample space and the training of the network, especially, how information from the preconditioned system can be used to increase reconstruction accuracy.

The sample space made has referred to the incremental learning method. The incremental learning may also be addressed in context of training data manipulation [35]. For example, in [36], an incremental learning strategy is implemented through the selection of the most informative training samples. Given enough data, an ANN will reconstruct the permittivities of materials and produce a more accurate result. The accuracy for reconstruction of permittivity depends on the amount of data available in these loss dielectric materials.

Before constituting the model the primary question is the production of samples. On the one hand, the characteristic of network should be considered; on the other hand, the sample data must do their best to reflect the intrinsic rule of materials permittivities. The learning strategy is implemented through the selection of most informative training samples [36]. The informativeness is defined as the sensitivity of the neural network output to perturbations in the input value of that pattern [37]. In [36], the output sensitivity vector is defined as (1),

$$\vec{S}_o^{(p)} = \left\| S_{oz}^{(p)} \right\|_2 \tag{1}$$

$\vec{S}_o^{(p)}$ is the output sensitivity vector, and $S_{oz}^{(p)}$ is the output-input layer sensitivity matrix. Each element $S_{oz,ki}^{(p)}$ of the sensitivity matrix is defined as a single output unit o_k to changes in the input vector $\vec{z}$; k

Figure 7. Structure of iron can.

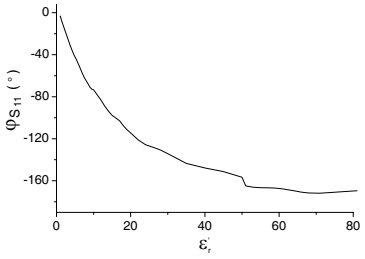

Figure 8. Phase variation of S-parameters due to the change in real part of permittivities at 2.45 GHz.

is the total number of output units.

$$S_{oz,ki}^{(p)} = \frac{\partial o_k}{\partial z_i^{(p)}} \tag{2}$$

In this paper, the FDTD is applied to simulate the $|S_{11}|$ and $\varphi_{S_{11}}$, using the real part and imagery part of different materials as input parameters. For example, Fig. 8 shows the phase variation of S-parameters due to the change in real part of permittivities. The slope of the curve which expresses the sensitivity of the output changes from small to large with the input data increasing. The slope is larger at the low permittivity material areas than the high permittivity material areas, and the samples in low permittivity material areas are more informative, so more samples have been selected in training neural networks. In addition, the low permittivity materials have larger relative errors with the same absolute reconstruction errors. The more samples have been selected, the better accuracy of reconstruction by BP neural network is. For example, when the real part of permittivity varies from 3 to 5, the sample intervals are 0.1. When the real part of permittivity varies from 5 to 10, the sample intervals are 0.2.

Thus, the relative errors of measurement for the materials permittivities are less than 5%.

6. THE RECONSTRUCTION RESULTS

The permittivity of material can be gained when the scattering parameters measured have been put in the trained BP network. So

Table 1. Effective permittivities of material at 2.45 GHz.

Material name	real part of permittivity			Imaginary part of permittivity		
	Measurement	Reference [38]	relative errors (%)	Measurement	Reference [38]	relative errors %
DMSO	46.890	48.900	−4.1	19.223	20.002	−3.9
Methanol	25.910	24.970	3.8	14.010	14.523	−3.5
Formic acid	6.839	7.135	−4.1	1.325	1.359	−2.5
Ethanol	8.680	8.939	−2.9	7.305	7.585	−3.7
Acetone	20.021	19.325	3.6	1.132	1.099	3.0
Glycol	19.576	18.969	3.2	17.489	16.898	3.5
Glycerin	6.909	7.123	−3.0	3.685	3.838	−4.0

Table 2. Effective permittivities of NaCl solutions with different fraction at 1 GHz.

ω (NaCl) (‰)	real part of permittivity			imaginary part of permittivity		
	measurement	reference [39]	relative error (%)	measurement	reference [39]	relative error (%)
5	82.72	79.85	3.5	16.87	17.57	−4.0
10	80.49	78.15	2.9	28.53	29.70	−3.9
20	77.75	74.89	3.7	54.70	53.17	2.9

the trained network can use the scattering parameter to measure the effective permittivity of materials quickly. Table 1 shows the reconstructed results of several organic solvents at 2.45 GHz. The accurate reconstructed results have been gained by BP network. Table 2 shows the reconstructed results of saline solution at 1 GHz, 15°C. The results show that the measurement apparatus can be used in a broadband measurement.

7. CONCLUSION

In this paper, we design an on-line measurement apparatus for materials permittivities. The new open-ended coaxial probe has been designed to measure the scattering parameters, and the techniques of BP neural network have been applied to reconstruct the permittivity. BP network is a simple, fast and convenient method to measure the permittivity of materials. The measured results show BP neural network can be applied to measurements of materials permittivities and work well. Moreover, the on-line measurement apparatus can be applied to measuring the material permittivities in a temperature rising process, because the iron can has a better thermal conductive property. The test probe is based on the open-ended coaxial line, which makes the measurement apparatus possible for broadband applications. Meanwhile, the measurement apparatus can be applied to measuring liquids, gases or powders. It can even perform measurements on the permittivity of chemistry reaction with time and temperature variation.

ACKNOWLEDGMENT

This project was supported by the National Science Foundation of China (No. 61001019).

REFERENCES

1. Addamo, G., G. Virone, D. Vaccaneo, R. Tascone, O. A. Peverini, and R. Orta, "An adaptive cavity setup for accurate measurements of complex dielectric permittivity," *Progress In Electromagnetics Research*, Vol. 105, 141–155, 2010.
2. Huang, K. and X. Yang, "A method for calculating the effective permittivity of a mixture solution during a chemical reaction by experimental results," *Progress In Electromagnetics Research Letters*, Vol. 5, 99–107, 2008.
3. Yan, L., K. Huang, and C. Liu, "A noninvasive method for determining dielectric properties of layered tissues on human back," *Journal of Electromagnetic Waves and Applications*, Vol. 21, No. 13, 1829–1843, Oct. 2007.
4. Chen, L. F., C. K. Ong, C. P. Neo, et al., *Microwave Electronics: Measurement and Materials Characterization*, John Wiley & Sons, West Sussex, England, 2004.
5. Hasar, U. C. and E. A. Oral, "A metric function for fast and accurate permittivity determination of low-to-high-loss materials from reflection measurements," *Progress In Electromagnetics Research*, Vol. 107, 397–412, 2010.
6. Meng, B., J. Booske, and R. Cooper, "Extended cavity perturbation technique to determine the complex permittivity of dielectric materials," *IEEE Trans. Microw. Theory Tech.*, Vol. 43, 2633–2636, 1995.
7. Kaatze, U., "Techniques for measuring the microwave dielectric properites of materials," *Metrologia,* Vol. 47, No. 2, S91–S113, 2010.
8. Baker-Jarvis, J., E. J. Vanzura, and W. A. Kissick, "Improved technique for determining complex permittivity with the transmission/reflection method," *IEEE Trans. Microw. Theory Tech.*, Vol. 38, No. 8, 1096–1103, 1990.
9. Hasar, U. C., "Permittivity determination of fresh cement-based materials by an open-ended waveguide probe using amplitude-only measurements," *Progress In Electromagnetics Research*, Vol. 97, 27–43, 2009.
10. Wang, Z., W. Che, and L. Zhou, "Uncertainty analysis of the rational function model used in the complex permittivity measurement of biological tissues using PMCT probes within a wide microwave frequency band," *Progress In Electromagnetics Research*, Vol. 90, 137–150, 2009.
11. Hasar, U. C., "Thickness-independent automated constitutive

parameters extraction of thin solid and liquid materials from waveguide measurements," *Progress In Electromagnetics Research*, Vol. 92, 17–32, 2009.

12. Zhang, H., S. Y. Tan, and H. S. Tan, "An improved method for microwave nonduetructive dielectric measurement of layered media," *Progress In Electromagnetics Research B*, Vol. 10, 145–161, 2008.
13. Le Floch, J. M., F. Houndonougbo, V. Madrangeas, D. Cros, M. Guilloux-Viry, and W. Peng, "Thin film materials characterization using TE modes," *Journal of Electromagnetic Waves and Applications,* Vol. 23, No. 4, 549–559, 2009.
14. Jin, H., S. R, Dong, and D. M. Wang, "Measurement of dielectric constant of thin film materials at microwave frequencies," *Journal of Electromagnetic Waves and Applications*, Vol. 23, No. 5–6, 809–817, 2009.
15. Valagiannopoulos, C. A., "On measuring the permittivity tensor of an anisotropic material from the transmission coefficients," *Progress In Electromagnetics Research B*, Vol. 9, 105–116, 2008.
16. Hasar, U. C. and O. Simsek, "An accurate complex permittivity method for thin dielectric materials," *Progress In Electromagnetics Research*, Vol. 91, 123–138, 2009.
17. Hasar, U. C., "Microwave method for thickness-independent permittivity extraction of low-loss dielectric materials from transmission measurements," *Progress In Electromagnetics Research*, Vol. 110, 453–467, 2010.
18. Kilic, E., F. Akleman, B. Esen, D. M. Ozaltin, O. Ozdemir, and A. Yapar, "3-D imaging of inhomogeneous materials loaded in a rectangular waveguide," *IEEE Trans. Microw. Theory Tech.*, Vol. 58, No. 5, 1290–1296, 2010.
19. Huang, K., X. Cao, C. Liu, and X.-B. Xu, "Measurement/computation of effective permittivity of dilute solution in saponification reaction," *IEEE Trans. Microw. Theory Tech.*, Vol. 51, No. 10, 2106–2111, 2003.
20. Luo, M., K. Huang, and T. Pu, "Measurement and prediction of dielectric for liquids based artificial nerve network," *ICMMT 2010 Proceedings*, 1083–1085, 2010.
21. Bartley, Jr., P. G., R. W. McClendon, and S. O. Nelson, "Permittivity determination by using an artificial neural network," *Instrumentation and Measurement Technology Conference, 1999. IMTC/99. Proceedings of the 16th IEEE*, Vol. 1, 27–30, 1999.
22. Eves, E. E., P. Kopyt, and V. V. Yakovlev, "Determination of

complex permittivity with neural networks and FDTD modeling," *Microwave and Optical Technology Letters*, Vol. 40, No. 3, 183–188, 2004.

23. Xu, Z.-B., R. Zhang, and W.-F. Jing, "When does online BP training converge?" *IEEE Transactions on Neural Network*, Vol. 20, No. 10, 1529–1539, 2009.
24. Liu, L., J. Chen, and L. Xu, "Realization and application research of BP neural network based on MATLAB," *2008 International Seminar on Future Biomedical Information Engineering*, 130–133, 2008.
25. Wang, S. and Y. Wang, "The demarcating method of infrared image measuring temperature based on GA-BP network," *2010 International Conference on Computer and Communication Technologies in Agriculture Engineering*, 2010.
26. Xuan, H. and M. He, "Study of detection technique simulation of high resolution radar based BP neural network," *Third International Conference on Natural Computation (ICNC2007)*, 2007.
27. Weckman, G. R., H. W. Paschold, et al., "Using neural networks with limited data to estimate manufacturing cost," *Journal of Industrial and Systems Engineering*, Vol. 3, No. 4, 257–274, 2010.
28. Gorriti, A. G. and E. C. Slob, "A new tool for accurate *s*-parameters measurements and permittivity reconstruction," *IEEE Transactions on Geosciences and Remote Sensing*, Vol. 43, No. 8, 1727–1735, 2005.
29. Ogasawara, E., L. C. Martinez, D. de Oliveira, et al., "Adaptive normalization: A novel data normalization approach for non-stationary time series," *Neural Networks (IJCNN), The 2010 International Joint Conference on Digital Object Identifier*, 1–8, 2010.
30. Akdemir, B., B. Oran, S. Gunes, et al., "Prediction of aortic diameter values in healthy turkish infants, children, and adolescents by using artificial neural network," *Journal of Medical Systems*, Vol. 33, No. 5, 379–388, 2009.
31. Sola, J. and J. Sevilla, "Importance of input data normalization for the application of neural networks to complex industrial problems," *IEEE Trans. Nuclear Science*, Vol. 44, No. 3, 1464–1468, 1997.
32. Holloway, A. and T. Chen, "Neural networks for predicting the behavior of preconditioned iterative solvers," *Proceedings of the 2007 International Conference on Computational Science*, Beijing, China, May 2007.

33. EI-Bakry, H. M. and Q. Zhao, "Fast pattern detection using normalized neural networks and cross-correlation in the frequency domain," *EURASIP Journal on Applied Signal Processing*, Vol. 13, 2054–2060, 2005.
34. Zhang, Q. J. and K. C. Gupta, *Neural Networks for RF and Microwave Design*, Artech House, Norwood, MA, 2000.
35. Wan, S. and L. E. Banta, "Parameter incremental learning algorithm for neural networks," *IEEE Transactions on Neural Network*, Vol. 17, No. 6, 1424–1438, 2006.
36. Engelbrecht, A. P. and R. Brits, "A clustering approach to incremental learning for feedforward neural networks," *Proc. Int. Joint Conf. Neural Netw.*, Vol. 3, 2019–2014, 2001.
37. Engekbrecht, A. P. and I. Cloete, "Incremental learing using sensitivity analysis," *Proc. Int. Joint Conf. Neural Netw.*, 380, USA, 1999.
38. Wei, H., X.-Q. Yang, K.-M. Huang, et al., "Study on the complex permittivity of common organic reagent at 2.45 GHz," *Chemical Research and Application*, Vol. 18, No. 10, 1232–1234, 2006.
39. Stogryn, A., "Equations for calculating the dielectric constant of saline water," *IEEE Trans. Microw. Theory Tech.*, Vol. 19, No. 8, 733–736, 1971.